



Full Length Article

Microarray Analysis of Nitric Oxide Responsive Transcripts in *Arabidopsis* Root G2/M Junction Cells

Miaomiao Li^{1†}, Tao Yao^{1†}, Fei Li^{1†}, Yaochuan Zhang² and Sulan Bai^{*}

¹College of Life Sciences, Capital Normal University, Beijing 100048, P.R. China

²Beijing Vocational College of Agriculture, Beijing 102422, P.R. China

*For correspondence: sulanb@sina.com; zzuliuqi@hotmail.com

†Contributed equally to this work

Abstract

Nitric oxide (NO) is an inevitable signaling molecule available throughout the plants life. In addition to its effects on each step of plant growth, it possibly has a key role in cell cycle. However, limited by the current understanding of the cell cycle, gene expression profiles of the G2/M junction cells in responses to NO remain limited. Regulation on gene expression in response to NO was investigated in root G2/M junction cells by applying whole genome ATH1 microarray analysis, which included more than 24,000 genes. We analyzed the effects of NO on G2/M junction cells isolated by fluorescent activated cell sorting (FACS) employing a G2/M definite transgenic reporter construct (*cycB1::GFP*) in Columbia wild-type (WT) and chlorophyll a/b combining proteins associated with (*cue1*) mutant (with high level endogenous NO) background. By comparing the gene expression under 20 μ M sodium nitroprusside (SNP) in WT background, 35 differentially expressed genes were observed. Thirty genes were up-regulated genes while five others down-regulated. Majority of genes were phytohormone-related. Their involvement in the cell cycles regulation, indicated that NO may regulate cell division through the regulation of phytohormone. By comparing the gene expression in the *cue1* background, it was noticed that 110 genes are differentially expressed. Thirteen genes were up-regulated while 97 down-regulated. A majority of genes were involved in metabolic regulation and stress response indicating that NO may aggravate metabolic disorder in *cue1* mutant. This research revealed the effects of NO on G2/M junction cells in *Arabidopsis* based on a whole genome microarray. These researchers provide essential insight into plant cell cycle and growth in response to NO. © 2019 Friends Science Publishers

Keywords: G2/M junction cells; Nitric oxide; Cell cycle; Fluorescent activated cell sorting; Phytohormones

Introduction

The gaseous nitric oxide (NO) is tiny, amphiphilic molecule having distinct functions in plants. The function of NO in plants ranges from root development, seed germination, and programmed cell death (Neill, 2005; Bai *et al.*, 2013; Signorelli and Considine, 2018; Sun *et al.*, 2018). It also protects from diseases, stomatal closure, and hormone responses and flower timing control (Desikan *et al.*, 2004; He *et al.*, 2004; Romero-Puertas *et al.*, 2004; Wendehenne *et al.*, 2004; Feng *et al.*, 2013; Arasimowicz-Jelonek and Floryszak-Wieczorek, 2014; Zhou and Zhang, 2014). An excessive amount of NO is toxic. It reduces growth and delays development in plants. The previous research showed retardation of root-growth during existence of a NO donor and sodium nitroprusside (SNP). The negative effect of SNP was found in a dose dependent manner and this effect repressed the root growth (He *et al.*, 2004). The presence of excessive NO is possibly due to cell cycle were detected at G2/M phase it was a major cause of retardation

of root growth (Bai *et al.*, 2012).

Transcriptional changes in *Arabidopsis* due to NO have been analyzed employing medium- and large-scale transcriptome analyses including microarray (Parani *et al.*, 2004), amplified cDNA with fragmented polymorphism (Polverari *et al.*, 2003) and real-time PCR (Huang *et al.*, 2002). NO can promote cell division in cell suspensions of alfalfa derived from leaf protoplast, and ephemerally induces CYCA2; 1 and CYCD3 including 1 expression of mRNA (Ötvös *et al.*, 2005), which positively regulate the transition from G0 to G1. NO maybe targeting G1 to S transition by down-regulated KRP gene and regulate lateral root initiation (Correa-Aragunde *et al.*, 2006). However, the effects of NO on mitotic cells have not been reported.

Nitric oxide hypersensitive mutant *cue1* exhibited root-growth hypersensitivity to NO (He *et al.*, 2004). The *cue1* mutant was detected while screening of genes that allows the activation of nuclear promoters based on phytochrome by controlling the chlorophyll, a/b binding protein de-repression, while three other promoters during

de-etiolation (Li *et al.*, 1995). Morphological phenotypes of *cue1* mutants include small plant size and reticulate leaves, having paraveins of dark green color and interveinal regions with light green. It was due to *cue1*, which showed a relatively higher level of endogenous and hypersensitive to NO. Furthermore, *cue1* reaction with NO is also different from WT. Their profiling differences of mitotic cells in responses to NO remain unknown.

The main goal of this research was to examine the effect of NO on mitotic cells. G2/M specific transgenic reporter construct (*cycB1::GFP*) in *cue1* and WT background were used because of their help to avoid from cell cycle arrest at G2/M phase (Bai *et al.*, 2012). The positive aspects of the microarray hybridization were undertaken for direct quantitative measurement and analysis in numerous transcripts, simultaneously (Li *et al.*, 2008; Wei *et al.*, 2011). A total of 22,500 probes representing about 24,000 sequences of Arabidopsis were part of the released ATH1 genome. The verification of changes in genome-scale transcript due to NO treatment was done (Li *et al.*, 2008). The transcript changes due to NO and their analysis provide a good evidence to elaborate its significant effects on plant cell cycle and root development in correspondence to NO.

Materials and Methods

Plant Stocks

Arabidopsis (*cue1*) seeds were gifted by Dr. J. Chory at Salk Institute. Arabidopsis plants (Columbia ecotype) containing the *cycB1::GFP* reporter construct was a gift from Peter Doerner. The *cycB1::GFP* reporter line with *cue1* background was crossed and selected in our laboratory. In this construct, Green fluorescent protein (GFP) encoded with translated region was merged with mitotic destruction box and was guided by Arabidopsis *cycB1* promoter; the reason why the GFP gene is emulated into late S phase at the beginning stage and the protein degraded in the mid M-phase.

Plant Growth Conditions

Growth chambers were used for growing plant under specific conditions such as, 20°C temperature maintained for 16 h/day and 8 h/night under cool white light. Surface sterilization of seeds was performed before placing them in growth chamber. Seeds were surface sterilized in specific conditions (rinsed in water, 20% bleach, and placed at 4°C for 3–4 days in dark places) for better results. Murishige and Skoog (MS) media (0.5×) made of (Sigma-Aldrich, St. Louis, MO, USA) was used as a platform for seeds. The seeds were overlaid carefully with 0.8% agar. The seeds under observation were arranged in rows at a specific density of ~600 seeds per row and grew on surface of nylon mesh square plates to harvest rapidly. Seedlings were grown

on media without SNP for five days. Then 20 μM SNP was added on the upper cover of each plates to harvest NO, and after a 24 h treatment, its important effects were studied.

Sample Collection

Root tips of about 3 mm in length were used for protoplasts preparation. Dissected root tips were placed in protoplasting solution (1.5% cellulase, 0.1% pectolyase, 600 mM Mannitol, 2 mM MgCl₂, 0.1% BSA 2 mM CaCl₂, 2 mM MES, 10 mM KCl, pH 5.5) according to Birnbaum's methods. Protoplasting solution placed in small light-resistant Petri dishes with 70 μm cell strainers inside and incubated for 60 to 90 min at 25°C with agitation at a speed of 85 rpm. The accumulated protoplast from Petri dishes was spun down at 350 rcf for concentrating cells better. The clear liquid on the surface of precipitation was aspirated, while cell pellet was dipped in 1 mL of iso-osmotic solution contains (600 mM Mannitol; 0.1% BSA, 2 mM MgCl₂, 2 mM CaCl₂, 2 mM MES, and 10 mM KCl, at pH 5.5). The cell suspension was filtered through a 70 μm then a 40 μm cell strainer.

Plant Protoplast Fluorescence Activated Cell Sorting (FACS)

GFP cells were set apart on FACS Vantage with the help of a small nozzle (100 μm size) at a rate of 2,000–5,000 events/s. The fluid pressure of 30 psi was used for sorting. Protoplasts from Columbia wild-type plants were non-GFP expressing and used as a negative control. GFP cells were elected on the basis of their green channel (~530 nm long) emission intensity and classified directly into lysis buffer (Qiagen RLT buffer). Moreover, it was properly mixed and immediately RNA was extracted and frozen at -80°C. Some cells gave fluorescence in the equal intensity of green and orange colors with lambda approx. 575 nm and it is very necessary to eliminate these cells to establish an autofluorescence filter. Total RNA was isolated using the Qiagen RNeasy Plant Mini kit (Valencia, California, United States) according to manufacturer's protocol.

Total RNA Preparation and Microarray Hybridization

RNA samples were processed as per recommendation of the manufacturer (Affymetrix, Santa Clara, CA, USA). Microarray hybridization was accomplished in Captial Bio Corporation, Beijing, China. In brief, in a Superscript II RT from company (Invitrogen, Carlsbad) and T7-(dT) 24 primer were used for the reverse transcription of 10 μg of total RNA. Each double-strand cDNA was synthesized from the first stranded cDNA. Phenol-chloroform extraction and ethanol precipitation process were utilized for the purification of Double-strand cDNA. After purification, Bio-Array High-Yield RNA Transcript Labeling Kit (Enzo Diagnostics, Farmingdale) made by USA was used for generation of biotin-labelled cRNA during *in vitro*

transcription reaction (IVT). RNeasy Mini Kit (Qiagen) was used for the purification reaction product of IVT and then properly quantified with Biophotometer (Brinkmann, USA). A 300 μ L of hybridization cocktail was prepared from the 15 μ g of fragmented of cRNA. To target hybridization 225 μ L of the cocktail, using ATH1 Genome Array (Affymetrix, Inc, USA), the hybridization was performed on the biotin-labelled targets to create to GeneChip from *Arabidopsis*. This process was done for 16 h at rpm of 60 in an Affymetrix GeneChip Hybridization Oven at 45°C. With the help of Affymetrix Fluidics Station 400 washing and staining process were achieved and then antibody amplification for eukaryotic targets (EuKGEWSv4) was performed. Finally, Affymetrix Scanner as used to scan the arrays.

Data Analysis

Affymetrix GeneChip operating software (GCOS) v1.2 was employed to import the raw data from microarray experiments for normalization. After normalization, the present (P), absent (A) calls and probe intensities of each chip were determined. To recognize the major variation in expression level of the genes, significance analysis of microarrays (SAM) was employed (Tusher *et al.*, 2001). Average-linkage hierarchical clustering was applied by using the CLUSTER program, and the results were displayed by using TREEVIEW. The GO analysis was done on the TAIR Web site (www.arabidopsis.org). The AtGenExpress data were retrieved from the international AtGenExpress repository and downloaded from LabArchives.https://mynotebook.labarchives.com/share_attachment/sulanb/MTYzNDIuM3wzMTUyNC8xMjU3MS0yL1RyZWVOb2RILzI2NjY1MzExNzB8NDE0ODQuMw==).

Real-time Polymerase Chain Reaction

Real-time PCR was executed with the help of SYBR Green/ROX qPCR Master Mix (Fermentas) on an iCycler iQ5 thermocycler (Bio-Rad). Each RNA sample was treated with RNase-free DNase I and First Strand cDNA was prepared using the RevertAid™ First Strand cDNA Synthesis Kit (Fermentas) with random primers according to the protocol. The First Strand cDNA Synthesis reaction mix (20 μ L) contained cDNA from 200 ng total RNA. The PCR included 5 min for 95°C, and 40 cycles of 30 s for 94°C, 30 s for 58°C, and 45 s for 72°C. After a cooling step, the melt curve was examined. The PCR results were quantified using the Pfaffl method as described in the RT-PCR applications guide (Bio-Rad).

Availability of Supporting Data

The original microarray data are available at https://mynotebook.labarchives.com/share_attachment/sulanb/MTYzNDIuM3wzMTUyNC8xMjU3MS0yL1RyZWVOb2RILzI2NjY1MzExNzB8NDE0ODQuMw==.

Results

Root Growth is Retarded in Response to NO

Our previous results showed that root growth was arrested in response to NO in a dose-dependent manner. To verify the effect of various NO concentrations on the transcriptional response, *Arabidopsis* roots of WT and *cue1* plants were divided into groups and growth on 0, 2, 4, 6, 8, 10, 20, 50, 100 and 200 μ M SNP medium.

Roots of WT and *cue1* without SNP were used as controls. The root length of WT plants grew on 0 and 2 μ M SNP medium was nearly identical. Root growth of *cue1* mutant was hindered severely on 2 μ M SNP medium. Root growth in *cue1* was 1/8 of the length of WT on 2 μ M SNP medium. On 20 μ M SNP medium, root growth of WT was only 1/3 length of the growth in control plants, while the roots of *cue1* plants did not elongate at all. On 50 μ M SNP medium, neither the roots of WT nor *cue1* plants elongated (Fig. 1). Therefore, 2 and 20 μ M SNP concentrations were applied to future experimental treatments on *cue1* and WT seedlings.

G2/M Junction Cells Collected by FACS

Our previous result showed that NO induces cell cycle arrest at G2/M point of the cell cycle. To assess the effects of NO on mitotic cells at G2/M junction, G2 specific transgenic reporter constructs (*cycB1::GFP*) in Col-0 wild-type and *cue1* background were used in this research (Fig. 2A B and C). In this construct, the translated region encoding the green fluorescent protein was fused to a mitotic destruction box and was driven by the *Arabidopsis cycB1* promoter. Thus, the *GFP* gene transcribes at the late S phase, and the protein is degraded in the mid-M phase. Enzymatic digestion was employed to prepare the root tip protoplasts. Moreover, FACS was then used to collect the GFP positive cells (Fig. 2D E F and G). Approximately 0.2 million cells from each sample were collected for transcription analysis (Fig. 2F and G). WEREWOLF (WER)::GFP is expressed in the none-hair cells of epidermis. For protoplast can be easily obtained from WER::GFP transgenic lines, therefore WER::GFP was used as positive control to testify our sorting system effectiveness (Fig. 2E). The mRNAs of collected GFP positive cells in each sample were analyzed with microarray.

Quantitative Real-time PCR Confirmed the Reliability of Microarray Data

Quantitative real-time (qRT)-PCR was used to confirm gene expression patterns observed from microarray. The complete RNA structure was separated from *Arabidopsis* root tips and subjected to first strand cDNA synthesis, qRT-PCR assays were performed with synthesized cDNAs.

In this study, 18S rRNA gene was used to quantitate transcript abundance. Several genes up-regulation were

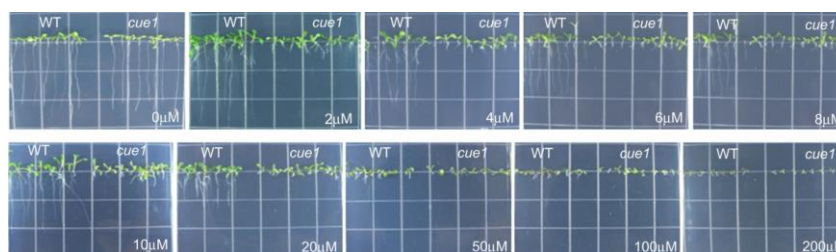


Fig. 1: Root growth in response to sodium nitroprusside (SNP) for Columbia wild type (WT) and *cue1*. Seeds were plated on the indicated concentrations

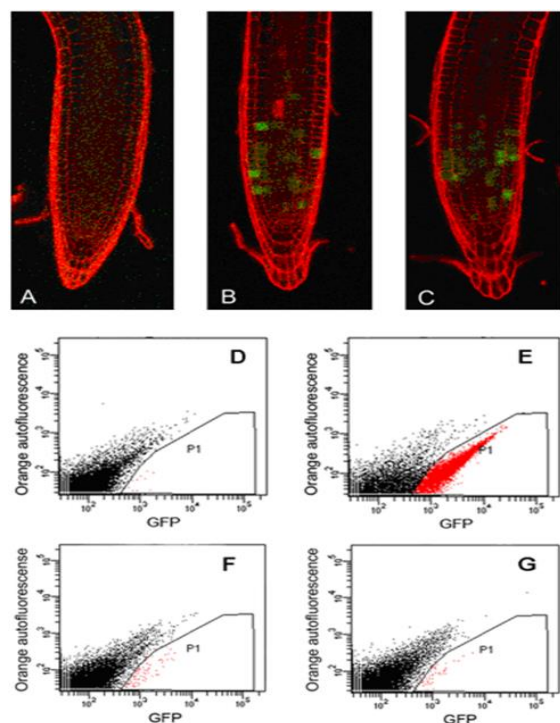


Fig. 2: Sorting *CycB1::GFP* cells from primary roots of 6-day-old *Arabidopsis* plants. Confocal image of a primary root in WT (A); Confocal image of a primary root in transgenic plant expressing *CycB1::GFP* in WT background (B); Confocal image of a primary root in transgenic plant expressing *CycB1::GFP* in *cue1* background (C). Biparametric analysis of protoplasts of the wild-type plants. Cells have a typical autofluorescence pattern of approximately equal fluorescence in the two channels (D); Biparametric analysis of protoplasts in the *Wer::GFP* plants (control). The dense cluster of target protoplasts, which are delimited by the sorting gate, emit more intensely in green than in red wavelengths. Those are GFP-positive target cells (E); FACS sorting of *CycB1::GFP* protoplasts from WT background (F); FACS sorting of *CycB1::GFP* protoplasts from *cue* background (G)

observed both in microarray and qRT-PCR, for example, *ACO1*, *ARL*, *ARaR3*, *AHP1*, and also genes down-regulation as well, *NR1*, *CPC* (Fig. 3). These five genes *ACO1*, *ARL*, *ARR3*, *AHP1* and *NR1* were selected randomly

for real-time PCR analysis (Fig. 3C and D). It indicated that the microarray hybridization and data analysis system were reliable.

Clustering Analysis and Functional Classification of the Differentially Expressed Genes

In G2/M cells of both WT and *cue1* mutant treated with NO, clustering analysis of differentially expressed genes was performed using average linkage clustering method (Fig. 4). The up-regulated genes are shown in red color and down-regulated genes in green color. The ratio of treated and untreated samples was plotted using log regression model (Table 1 and 2).

In G2/M cells of WT, a total of 35 differentially expressed genes were identified following treatment with NO, with 30 genes up-regulated and five down-regulated. Among these genes, we detected some phytohormone-related genes, as well as genes functioning in cell cycle regulation, stress response, and transcriptional mechanisms (Table 1).

There were 110 differentially expressed genes in NO-treated G2/M cells with *cue1* background. Thirteen genes were up-regulated and 97 down-regulated (Table 2). Global analysis showed that these genes function in metabolism, stress response, hormone signaling, and microbial resistance.

Functional Category of Differentially Expressed Genes

According to cellular components, biological process and molecular function, alternation in genes expression showed that a large number of genes expressed in wild-type and *cue1* mutant in response to NO were obviously different (Fig. 5). A homology search in Gene Ontology preformed functional classification of differential gene expression was done in WT and *cue1* mutants treated with NO and GO EASY databases. Functional annotation was made with KEGG database and TAIR as a reference. Differentially expressed genes are involved in a wide variety of functions, including those involved in hormone-secretion, stress response, transcription, and metabolic process. Some genes have no function annotation and hypothetical protein genes were classified as unknown functional genes (Table 3).

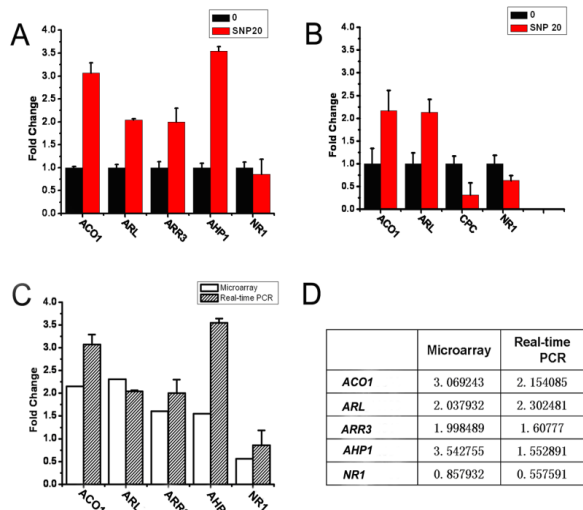


Fig. 3: Quantitative RT-PCR analysis of gene expression changes and comparison with microarray hybridization. Gene expression changes response to NO treatment in *CycB1::GFP* in WT background (A) and in *cue1* background (B). Transcript abundance of selected genes differently expressed between NO-treated and untreated plants (C). Exactly changes according to C results (D). Plants were treated with 20 μ M SNP for 24 h. The transcript levels of tested genes were normalized to that of 18S and relative expressions were compared with that of 7-d-old WT seedling without SNP treated. Means values were obtained from there independent PCR amplification. Error bars indicate SE

Genes Involved in Hormone Singaling Change Their expression in Response to NO

Three cytokinin-mediated genes were up-regulated in WT in the presence of NO, including A-type response regulator *ATRR3* and *ARR8* in cytokinin signaling pathway, and phosphotransferase protein *AHP1*. As a result, NO may participate in the cytokinin signaling pathway during root growth and development. NO led to the adventitious root formation mediating by auxin. Our microarray data indicated that two auxin-related genes *ARGOS* and *MONOPTEROS* were up-regulated. Expression of *MP* depends on the regulation of auxin that plays a critical role during *Arabidopsis* embryogenesis. *ARGOS* and *ARGOS-LIKE* were up-regulated. Those genes were well studied in auxin and brassinolide mediated cell division, organelle organization and cell expansion. While in *cue1* mutant, after treated with NO, GA-inducible gene *CYSTEINE PROTEINASE 1*, encoding a putative Cys proteinase, was up-regulated. *PP2CA* encodes a protein phosphatase 2C, that is a negative regulator of the ABA. Lastly, *JAS1* is a jasmonate response gene that was up-regulated.

Also, Ca^{2+} regulated protein kinase *CIPK1*, which functions in controlling ABA-dependent and independent stress in *Arabidopsis*, was up-regulated in this study. *BT2* encodes a BTB (BR-C, ttk and bab) protein, mediates multiple responses to nutrient depletion, stresses and hormones, was also down-regulated.

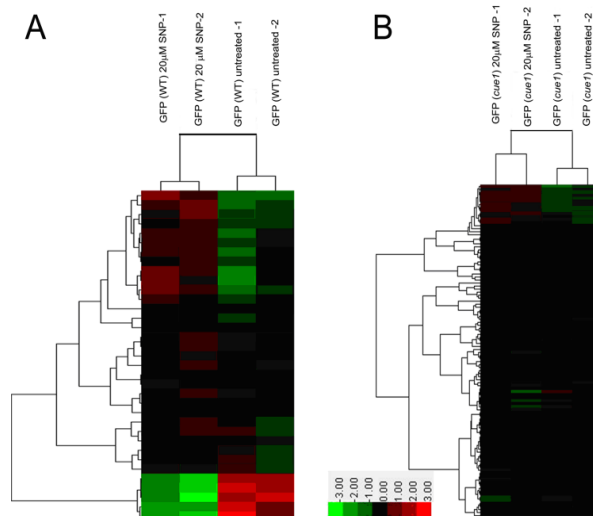


Fig. 4: Hierarchical clustering. Hierarchical clustering of up and down regulated genes in G2/M junction cells in WT (A) and in *cue1* background (B) in response to 20 μ M SNP treatment

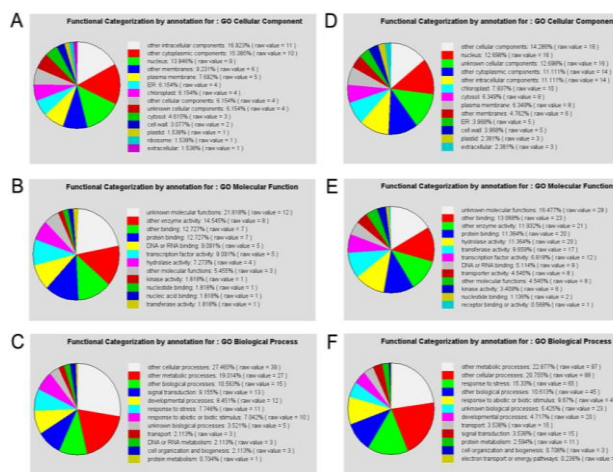


Fig. 5: Functional classifications from GO annotation. Functional classifications display classification and distribution of differentially expressed genes in response to SNP treatment. Genes with the regulation ratio of $\text{Log}_2 > 1.5$ or < -0.5 were selected. The Pearson's correlation coefficient for each experiment is listed. Panels show functional classifications from GO annotation organized by cellular component (A), biological process (B) and molecular function (C) in WT. GO annotation organized by cellular component (D), biological process (E) and molecular function (F) in *cue1* background

Positive Regulatory Genes in Cell Cycle Changed Their Expression

There are some genes related to the cell cycle or cell division that are independent on the direct or indirect involvement of NO in signal transduction events. The function of *E2F* transcription factor is well studied. It plays a crucial role in cell cycle progression. *E2F1* overexpression induces S-phase specific gene expression; thereby promote

Table 1: List of genes up and down-regulated in response to NO in G2/M cells in WT background

Public ID	Description	Gene Name	Log Ratio
Up-regulated Genes			
At3g59900	Auxin-regulated gene involved in organ size	ARGOS	1.341751
At1g19850	Auxin-regulated transcription factor	MP	0.649279
At2g41310	A-type response regulator involved in cytokinin-mediated signalling	ATRR3	0.719796
At1g59940	A-type response regulator induced by cytokinin	ARR3	0.685061
At3g21510	histidine phosphotransfer proteins, regulators of cytokinin signaling	AHP1	0.634957
At2g44080	involved in cell expansion-dependent organ growth, upregulated by brassinosteroid	ARL	1.203189
At1g25560	RAV transcription factor family, ethylene signaling	---	0.587317
At1g33590	disease resistance protein-related	---	0.82691
At1g69930	glutathione transferase	ATGSTU11	0.968546
At2g19590	1-aminocyclopropane-1-carboxylate oxidase	ACO1	1.107075
At5g20230	blue copper binding protein	ATBCB	1.083606
At1g66200	glutamine synthetase	ATGSR2	1.069733
At1g76470	cinnamoyl-CoA reductase, putative	---	0.72784
At4g24340	phosphorylase family protein	---	0.682736
At2g43140	transcription factor	---	1.042942
At2g22880	VQ motif-containing protein	---	0.983765
At1g54030	GDSL-motif lipase, putative	---	0.59774
At2g47260	WRKY transcription factor	WRKY23	0.593829
At1g71400	receptor like protein 12	AtRLP12	0.814291
At4g38410	dehydrin, putative	---	0.916293
At5g64905	Elicitor peptide 3 precursor	PROPEP3	0.799961
At4g11360	RING-H2 finger protein	RHA1B	0.705901
At1g14870	unknown	---	1.051573
At1g19020	unknown	---	0.78798
At2g26530	unknown	---	0.767303
At5g65300	unknown	---	0.675739
At5g60630	unknown	---	0.625757
At1g70420	unknown	---	0.617998
At3g18560	unknown	---	0.597994
Down-regulated Genes			
At1g77760	nitrate reductase	NR1	-0.84272
At5g22220	E2F transcription factors	E2F1	-0.87545
At1g05160	ent-kaurenoic acid hydroxylase	CYP88A3	-0.61172
At5g64080	lipid transfer protein	---	-0.75172
At4g02460	unknown	---	-0.6362

the progression of cell division. In this study, *E2F1* was down regulated. NO also promoted adventitious root development by regulating expression of *CYCD3*; *1* and *KPR2* during the cell cycle process.

Nitrate Metabolic Process

NR1 is a crucial component of disease resistance and is also regulated via S-nitrosylation. It was down-regulated in this study. NO can clearly be produced by NR activity, and NR1 deficiency can also disturb nitrogen assimilation. *ATGSR2* was regulated, it encodes a cytosolic glutamate synthetase, and potentially involved in nitrate metabolic process. Through these pathways, N-associated primary and secondary metabolism were both influenced by NO exposure.

Response to Stress

Plants induce stress-related genes to cope with environmental changes. In WT microarray data, up-regulation of *AtBCB* genes was noted following NO induction. Arabidopsis stellacyanin *AtBCB* is involved in oxidative stress response caused by aluminum. In *cue1* mutants, a large number of stress-related genes were

changed. *AtMPK3* was down regulated. *AtMPK3* alters its phosphorylation status by transmitting and receiving MAPK cascade signals and *AtMPK3* expression to collect the response by simulating the different environments. *NPR3* (*At5g45110*) was down-regulated in *cue1* when treated with NO. It might have a similar relationship with the disease resistance responses. Furthermore, pathogenesis-related gene Peroxidase 44 was strongly up-regulated by potassium-deficiency in WT. However, these genes were down-regulated in *cue1* mutant. Interestingly, these stress-related genes involved in disease resistance and wound healing were regulated differently in WT and *cue1* mutants coping with NO exposure.

Transcriptional Regulation

Most transcription factors bind to individual elements in DNA and either positively or negatively influences gene expressions. We found up-regulation of *WRKY* genes, *WRKY23* and *WRKY40*, both in WT and *cue1* mutants in response to NO. *WRKY23* is an auxin-induced gene and behaves as a downstream of Aux/IAA protein SOLITARY-ROOT (SLR)/IAA14 (INDOLE-3-ACETIC ACID INDUCIBLE 14).

Table 2: List of genes up and down-regulated in response to the NO in G2/M cells in cue1 background

Public ID	Description	Gene Name	Log Ratio
Up-regulated Genes			
At3g59900	Auxin-regulated gene involved in organ size	ARGOS	1.506045
At5g43700	auxin-induced protein AUX2-11	ATAUX2-11	0.684071
At2g41310	A-type response regulator involved in cytokinin-mediated signalling	ATRR3	0.65269
At2g44080	involved in cell expansion-dependent organ growth, upregulated by	ARL	1.005189
At3g23150	ethylene receptor, putative	ETR2	0.679735
At5g25350	EIN3-binding F-box protein 2	EBF2	0.839239
At2g19590	1-aminocyclopropane-1-carboxylate oxidase	ACO1	0.610458
At3g18000	methyltransferase, putative	NMT1	0.592284
At5g05900	glucuronosyl transferase-like protein	---	0.694159
At2g25160	putative cytochrome P450	CYP82F1	0.84133
At2g43140	transcription factor	---	0.689878
At3g17990	unknown	---	0.896328
At5g02550	unkown	---	0.591986
Down-regulated Genes			
Enzyme			
At1g05160	ent-kaurenoic acid hydroxylase	CYP88A3	-0.58542
At1g76150	enoyl-CoA hydratase	---	-0.58716
At5g59480	haloacid dehalogenase-like hydrolase	---	-0.58796
At4g36880	cysteine proteinase1	CP1	-0.5941
At5g59220	phosphatase, putative	PP2C	-0.6019
At3g57070	glutaredoxin family protein	---	-0.6022
At1g17180	glutathione transferase	ATGSTU25	-0.61952
At3g10720	pectinesterase, putative	---	-0.62691
At2g35710	glycogenin glucosyltransferase	---	-0.63211
At4g24160	lysophosphatidic acid acyltransferase	---	-0.64009
At2g28760	UDP-XYL synthase	UXS6	-0.68833
At5g16570	glutamine synthetase	GLN1;4	-0.71685
At5g24070	peroxidase-like protein	---	-0.71958
At1g64970	gamma-tocopherol methyltransferase	G-TMT	-0.76107
At1g78210	hydrolase	---	-0.76652
At1g78340	glutathione transferase	ATGSTU22	-0.84326
At5g11110	sucrose-phosphate synthase, putative	ATSPS2F	-0.89332
At1g06120	fatty acid desaturase family protein(mei)	---	-0.94193
nad3	NADH dehydrogenase subunit 3 protein	---	-0.95438
At1g05010	1-aminocyclopropane-1-carboxylate oxidase	EFE	-1.00787
At1g47600	myrosinase	---	-1.06596
At3g44860	farnesoic acid carboxyl-O-methyltransferase	FAMT	-1.24746
At1g50060	Aminotransferase	---	-1.27626
At1g77760	nitrate reductase	NR1	-1.5947
Stress-related			
At5g05410	transcription factor	DREB2A	-0.64405
At1g08830	superoxide dismutase	CSD1	-0.65646
At1g72520	lipoxygenase, putative	---	-0.67239
At4g36040	heat shock protein	---	-0.71703
At3g22830	heat stress transcription factor	AT-HSFA6B	-0.71898
At3g48360	putative protein MEL-26	BT2	-0.73681
At2g39350	ABC transporter family protein	---	-0.92465
At3g45640	mitogen-activated kinase	ATMPK3	-0.92791
At4g27400	late embryogenesis abundant protein	---	-1.00097
At1g53540	small heat shock protein	---	-1.19802
At5g12030	small heat shock protein	---	-1.27492
At4g25200	small heat shock protein	---	-0.84675
Response to wounding			
At1g20510	4-coumarate-CoA ligase	OPCL1	-0.65449
At5g13220	response to jasmonic acid	JAS1	-0.67758
At5g47240	mutT domain protein-like	ATNUDT8	-0.75468
At4g10270	wound-responsive family protein	---	-1.36339
Disease resistance			
At5g45110	regulatory protein NPR1-like	NPR3	-0.72805
At4g36010	pathogenesis-related protein	---	-0.75644
At4g12720	ADP-ribose hydrolase	AtNUDT7	-0.83819

Table 2: Continued

Table 2: Continued

Transcription regulation			
At2g46410	MYB transcription factor	CPC	-0.61842
At2g22630	MADs domain-containing protein	AGL17	-0.63812
At2g27310	F-box family protein	---	-0.6493
At1g44830	transcription factor	---	-0.65692
At1g80840	transcription factor	WRKY40	-0.72789
At4g37850	basic helix-loop-helix family protein(TF)	---	-0.88328
At3g16280	transcription factor	---	-0.95606
At4g04840	transcriptional regulator, putative	---	-0.91586
Hormone-related			
At4g12550	Auxin-Induced in Root cultures	AIR1	-1.30837
At2g44840	transcription factor	ATERF13	-0.65325
Others			
At1g52070	jacalin lectin family protein	---	-0.65856
At2g36950	metal ion binding protein	---	-0.87628
At4g30290	hydrolase	ATXTH19	-0.882
At5g01600	ferretin protein induced by nitric oxide	ATFER1	-0.92656
At1g78000	sulfate transporter	SULTR1;2	-0.96055
At1g08430	Al-activated malate efflux transporter	ALMT1	-0.98588
At3g06420	microtubule binding	ATG8H	-0.68033
At5g54840	Monomeric G protein	---	-0.68785
At3g46280	protein kinase-related	---	-0.69259
At1g12740	cytochrome P450, putative	CYP87A2	-0.70255
At3g17510	CBL-interacting protein kinase	CIPK1	-0.72856
At3g04320	trypsin inhibitor, putative	---	-0.75236
At3g51660	macrophage migration inhibitory factor family protein	---	-0.80296
At1g76640	calmodulin-related protein, putative	---	-0.9048
At1g27770	Ca ²⁺ -ATPase	ACA1	-0.60276
At3g16440	myrosinase binding protein, putative	---	-0.99316
At3g02550	LOB DOMAIN-CONTAINING PROTEIN 41	LBD41	-1.36118
At5g47450	Tonoplast intrinsic protein(NH3)	AtTIP2;3	-0.63881
orf135b	orf135b	orf135b	-0.59925
orf118	hypothetical protein	orf118	-0.79592
orf114	hypothetical protein	orf114	-1.26723
Unkown			
At2g34070	unknown	---	-0.60241
At5g63130	unknown	---	-0.61016
At2g28400	unknown	---	-0.61072
At5g22580	unknown	---	-0.62683
At3g12320	unknown	---	-0.63058
At5g14730	unknown	---	-0.67374
At1g48330	unknown	---	-0.67793
At5g13190	unknown	---	-0.69079
At4g00770	unknown	---	-0.71619
At2g38870	unknown	---	-0.72038
At3g10020	unknown	---	-0.73148
At3g20340	unknown	---	-0.73335
At1g80240	unknown	---	-0.75535
At1g24440	unknown	---	-0.76883
At1g74950	unknown	---	-0.82007
At5g43580	unknown	---	-0.86782
At3g49190	unknown	---	-0.89527
At5g60530	unknown	---	-0.90817
At1g49700	unknown	---	-0.94786
At5g65660	unknown	---	-1.10463
At2g33790	unknown	---	-1.95228
At5g54370	unknown	---	-1.69253

CPC encodes a protein with a Myb-like factor. It evaluates the fate of epidermal cell differentiation and controls the root's hair growth in Arabidopsis root base. In *cue1* mutants, *CPC* was down-regulated. It also acknowledged us to get an insight into the function of NO in root hair development (Unpublished). *AGL17* acts in the photoperiod pathway of Arabidopsis. It was down-regulated

in this research. *AGL17* had been reported in promoting flowering via regulation of *LFY* and *API*.

Metabolic Process

More than 22% of secondary genes were altered in response to NO in *cue1* mutant. Metabolic processes are essential to

Table 3: Functional category of the differentially expressed genes

Genes	G2/M cells in WT		G2/M cells in <i>cue1</i>	
	Number	Percentage (%)	Number	Percentage (%)
Hormone-related	7	20	17	15.45
cell cycle	1	2.85	0	0
Nitrate metabolic process	2	5.7	0	0
response to stress	6	17.14	27	5.45
Transcription regulation	4	11.42	8	7.27
secondary metabolic process	3	8.57	6	5.45
others	7	20	35	31.81
unknown	8	22.86	22	20

ensure plant development and its adaptation to the environment. NO could up-regulate *AtGSTU11* in WT, which functions in lection synthesis. *ATGSTU25* and *AtGSTU22*, belonging to the tau class of GSTs, was down-regulated in *cue1* mutants. *CYP88A3* was down-regulated in WT as well as *cue1* mutants.

Others Genes

AtACO1 was up-regulated. It was mainly expressed in tip and maturation zone of Arabidopsis roots involved in brassinosteroids induced inhibition of root growth. It also functions in ethylene synthesis. *AtRLP12*, play a role in maintaining short stem cell. It was also up-regulated. We also found some genes with unknown function in G2/M junction of the cell cycle in response to NO.

Discussion

This study provides the details about the expression of substantial number of genes that are modulated by NO at the transcriptional level in WT and *cue1* root mitosis cells in Arabidopsis. The changes in gene expression in response to NO were different. NO inhibits the growth of Arabidopsis roots through the cell cycle arrest and decrease the meristematic cell number (Bai *et al.*, 2012). Transcriptional regulations play essential roles in controlling cell cycle progression. This research show that key cell cycle regulatory gene E2F was down-regulated in WT, which is consistent with the result of NO suppressing cell cycle. However, in *cue1* mutant, we did not find the expression change of cell cycle genes.

Both in WT and *cue1* mutant, the genes in hormone synthesis and signaling pathways were regulated obviously including auxin, cytokinin, gibberellin, ethylene and brassinosteroid, which was consistent with the previous reports (Feng *et al.*, 2013; Liu *et al.*, 2018; Lv *et al.*, 2018; Signorelli and Considine, 2018). NO inhibits cell cycle progression may relate to hormones. Recent studies show that NO can affect PIN1 protein levels in root tip cells, thereby decrease the PIN1-dependent auxin response in the apical organization, and inhibit apical cell division and reduce apical meristem size. We speculate that NO inhibits cell cycle processes mainly through indirect manners, and

which was regulated by a variety of plant hormones.

In *cue1* mutant, we found that, beside the phytohormone-related genes, differentially expressed genes most involved in secondary metabolism, stress response, disease resistance and transcriptional regulation. A large number of metabolic genes were found indicating NO may aggravate metabolic disorder in *cue1* mutant. The *cue1* mutant has higher concentration level of nitric acid. Furthermore, it is also diminished during the mesophyll and chloroplast development (Li *et al.*, 1995; Voll *et al.*, 2003). These defects associated with these organelles can lead to discharge the reactive oxygen species (ROS) and disorder its metabolic pathway (Noronhadutra *et al.*, 1993). On the other hand, the import of phosphoenolpyruvate (PEP) from the cytosol into the plastid stroma is catalyzed by phosphoenolpyruvate/phosphate translocator 1 (PPT1) that is defective in *cue1* mutant (Streatfield *et al.*, 1999; Knappe *et al.*, 2003). PEP plays a central role in plant metabolism and it can be delivered by the PPT from the cytosol or may be generated inside the plastids by a complete glycolytic pathway (Fischer *et al.*, 1997). An excessive amount of NO may retard its metabolic pathway and repress root growth.

The differential expressions were observed frequently in genes with unknown function in response to NO treatment. Moreover, some additional are compulsory to verify the NO work model and its functioning mechanisms further. High-throughput transcriptional profiling technology has been successfully employed to discuss the influence of NO on gene expression in plants (Parani *et al.*, 2004). However, the influence of NO on specific cell types is still not reported. This study reported the transcriptional profiling of NO on the mitosis cells at G2/M phase, which will be very useful to understand NO's functions on cell cycle regulation and plant development.

Conclusion

The variations in gene expression in correspondence to NO were different in WT and *cue1*. In WT background, NO exerted its function by regulating phytohormone-related genes including auxin-regulated genes, cytokinin-mediated signaling pathway genes, brassinosteroid-regulated genes, ethylene signaling genes and E2F transcription factors indicating that NO is taking part in regulation of cell

division through the regulation of phytohormone related genes and cell cycle regulator. While in the *cue1* background, we found that differentially expressed genes most involved in secondary metabolism, stress response, disease resistance and transcriptional regulation besides phytohormone-related genes. A large number of metabolic genes were found, indicating NO may aggravate metabolic disorder in *cue1* mutant. On the other hand, *cue1* mutant contains a high concentration of endogenous NO, may affected in mesophyll and chloroplast. Moreover, it leads to defective PPT1 that may lead to hypersensitivity to NO and metabolic disorder. These results provide important insight onto plant cell cycle and development in response to NO.

Acknowledgments

National Natural Science Foundation of China supported this research work (No. 30771094, 31270821), Beijing Natural Science Foundation (No. 5112006).

References

- Arasimowicz-Jelonek, M. and J. Floryszak-Wieczorek, 2014. Nitric oxide: an effective weapon of the plant or the pathogen. *Mol. Plant Pathol.*, 15: 406–416
- Bai, S., M. Li, T. Yao, H. Wang, Y. Zhang, L. Xiao, J. Wang, Z. Zhang, Y. Hu, W. Liu and Y. He, 2012. Nitric oxide restrains root growth by DNA damage induced cell cycle arrest in *Arabidopsis thaliana*. *Nitric Oxide – Biol. Chem.*, 26: 54–60
- Bai, S., T. Yao, M. Li, X. Guo, Y. Zhang, S. Zhu and Y. He, 2013. PIF3 is involved in the primary root growth inhibition of *Arabidopsis* induced by nitric oxide in the light. *Mol. Plant*, 7: 616–625
- Correa-Aragunde, N., M. Graziano, C. Chevalier and L. Lamattina, 2006. Nitric oxide modulates the expression of cell cycle regulatory genes during lateral root formation in tomato. *J. Exp. Bot.*, 57: 581–588
- Desikan, R., M. Cheung, J. Bright, D. Henson, J.T. Hancock and S.J. Neill, 2004. ABA, hydrogen peroxide and nitric oxide signalling in stomatal guard cells. *J. Exp. Bot.*, 55: 205–212
- Feng, J., C. Wang, Q. Chen, H. Chen, B. Ren, X. Li and J. Zuo, 2013. S-nitrosylation of phosphotransfer proteins represses cytokinin signaling. *Nat. Commun.*, 4: 1529
- Fischer, K., B. Kammerer, M. Gutensohn, B. Arbing, A. Weber and R.E. Häusler, 1997. A new class of plastidic phosphate translocators, a putative link between primary and secondary metabolism by the phosphoenolpyruvate/phosphate antiporter. *Plant Cell*, 9: 453–462
- He, Y., R.H. Tang, Y. Hao, R.D. Stevens, C.W. Cook, S.M. Ahn, L. Jing, Z. Yang, L. Chen and F. Gu, 2004. Nitric oxide represses the *Arabidopsis* floral transition. *Science*, 305: 1968–1971
- Huang, X., U. von Rad and J. Durner, 2002. Nitric oxide induces transcriptional activation of the nitric oxide-tolerant alternative oxidase in *Arabidopsis* suspension cells. *Planta*, 215: 914–923
- Knappe, S., T. Löttgert, A. Schneider, L. Voll, U. Flügge and K. Fischer, 2003. Characterization of two functional phosphoenolpyruvate/phosphate translocator (PPT) genes in *Arabidopsis*—AtPPT1 may be involved in the provision of signals for correct mesophyll development. *Plant J.*, 36: 411–420
- Li, H., K. Culligan, R.A. Dixon and J. Chory, 1995. CUE1: A mesophyll cell-specific positive regulator of light-controlled gene expression in *Arabidopsis*. *Plant Cell*, 7: 1599–1610
- Li, L., H. He, J. Zhang, X. Wang, S. Bai, V. Stolc, W. Tongprasit, N.D. Young, O. Yu and X.W. Deng, 2008. Transcriptional analysis of highly syntenic regions between *Medicago truncatula* and *Glycine max* using tiling microarrays. *Genom. Biol.*, 9: R57
- Liu, M., H. Zhang, X. Fang, Y. Zhang and C. Jin, 2018. Auxin acts downstream of ethylene and nitric oxide to regulate magnesium-deficiency-induced root hair development in *Arabidopsis thaliana*. *Plant Cell Physiol.*, 59: 1452–1465
- Lv, X., H. Li, X. Chen, X. Xiang, Z. Guo, J. Yu and Y. Zhou, 2018. The role of calcium-dependent protein kinase in hydrogen peroxide, nitric oxide and aba-dependent cold acclimation. *J. Exp. Bot.*, 69: 4127–4139
- Neill, S., 2005. NO way to die – nitric oxide, programmed cell death and xylogenesis. *New Phytol.*, 165: 5–8
- Noronhadutra, A.A., M.M. Epperlein and N. Woolf, 1993. Reaction of nitric-oxide with hydrogen-peroxide to produce potentially cytotoxic singlet oxygen as a model for nitric oxide-mediated killing. *FEBS Lett.*, 321: 59–62
- Ötvös, K., T.P. Pasternak, P. Miskolczi, M. Domoki, D. Dorjgotov, A. Szűcs, S. Bottka, D. Dudits and A. Fehér, 2005. Nitric oxide is required for, and promotes auxin-mediated activation of, cell division and embryogenic cell formation but does not influence cell cycle progression in alfalfa cell cultures. *Plant J.*, 43: 849–860
- Parani, M., S. Rudrabhatla, R. Myers, H. Weirich, B. Smith, D.W. Leaman and S.L. Goldman, 2004. Microarray analysis of nitric oxide responsive transcripts in *Arabidopsis*. *Plant Biotechnol. J.*, 2: 359–366
- Polverari, A., B. Molesini, M. Pezzotti, R. Buonaurio, M. Marte and M. Delledonne, 2003. Nitric oxide-mediated transcriptional changes in *Arabidopsis thaliana*. *Mol. Plant-Microb. Interac.*, 16: 1094–1105
- Romero-Puertas, M.C., M. Perazzolli, E.D. Zago and M. Delledonne, 2004. Nitric oxide signalling functions in plant–pathogen interactions. *Cell. Microbiol.*, 6: 795–803
- Signorelli, S. and M.J. Considine, 2018. Corrigendum: Nitric oxide enables germination by a four-pronged attack on ABA-induced seed dormancy. *Front. Plant Sci.*, 9: 654
- Streatfield, S.J., A. Weber, E.A. Kinsman, R.E. Hausler, J. Li and D. PostBeittenmiller, 1999. The phosphoenolpyruvate/phosphate translocator is required for phenolic metabolism, palisade cell development and plastid-dependent nuclear gene expression. *Plant Cell*, 11: 1609–1621
- Sun, H., F. Feng, J. Liu and Q. Zhao, 2018. Nitric oxide affects rice root growth by regulating auxin transport under nitrate supply. *Front. Plant Sci.*, 9: 659
- Tusher, V.G., R. Tibshirani and G. Chu, 2001. Significance analysis of microarrays applied to the ionizing radiation response. *Proc. Natl. Acad. Sci. USA*, 98: 5116–5121
- Voll, L., R.E. Hausler, R. Hecker, A. Weber, G. Weissenböck, G. Fiene, S. Waffenschmidt and U. Flügge, 2003. The phenotype of the *Arabidopsis cue1* mutant is not simply caused by a general restriction of the shikimate pathway. *Plant J.*, 36: 301–317
- Wei, L.Q., L.F. Yan and T. Wang, 2011. Deep sequencing on genome-wide scale reveals the unique composition and expression patterns of microRNAs in developing pollen of *Oryza sativa*. *Genom. Biol.*, 12: R53
- Wendehenne, D., J. Durner and D.F. Klessig, 2004. Nitric oxide: a new player in plant signalling and defence responses. *Curr. Opin. Plant Biol.*, 7: 449–455
- Zhou, K. and J. Zhang, 2014. Nitric oxide in plants and its role in regulating flower development. *Yi Chuan*, 36: 661–668

(Received 06 June 2018; Accepted 21 June 2018)